Physica D 61 (1992) 197–204
North-Holland

PHYSICA D

Localized phenomena during spatio-temporal intermittency in directional viscous fingering

S. Michalland and M. Rabaud

Laboratoire de Physique Statistique de l'Ecole Normale Supérieure, associé au CNRS et aux Universités Paris VI et VII, 24 rue Lhomond, 75231 Paris Cedex 05, France

In the directional viscous fingering instability, the interface can evolve from a basic steady state to chaos by spatio-temporal intermittency. One essential feature of such a transition is that the chaotic domains appear by a contamination process of the steady phase. This mechanism is investigated here and it is shown that contamination occurs by two localized structures: dilatation waves and pairs of static asymmetric cells. These two structures suggest an elastic behaviour of the pattern.

1. Introduction

Nonlinear dynamics of pattern-forming systems has been an important center of interest since a few years. Recently many studies have been devoted to the simplest case of one dimensional systems. For such 1D systems, one possible transition to chaos has been described theoretically in terms of spatio-temporal intermittency (STI) [1] and studied experimentally in convection [2] and in directional viscous fingering (also called the printer's instability) [3]. In this transition, ordered domains coexist with chaotic ones and the averaged fraction of chaotic occupation depends on one control parameter. Another characteristic feature is that chaos results from an invasion of the ordered domains by nearby chaotic domains (i.e. chaos never appears isolated in the middle of an ordered area). Therefore a local description of the contamination mechanisms is as essential as a statistical description for the understanding of the STI. In the present article, we show that the contamination occurs either by localized traveling waves or by motionless pairs of asymmetrical cells. These two structures, already observed during transients [4] suggest that the pattern has an elastic behaviour, the characteristics of which can be measured.

2. The basic instability

The printer's instability is a viscous fingering experiment [5]. It appears in a journal-bearing geometry, and was first described by Pitts and Greiller [6] and Taylor [7]. We revisited this instability in a new configuration which allows to reach a variety of non linear behaviours of the interface and in particular a STI regime [3]. In the gap between two off-centered cylinders a small amount of silicon oil is set (minimum gap $b_0 < 1$ mm, radius of cylinders 33 and 50 mm). The cylinders can rotate independently and we call the tangential velocities of the inner and outer cylinder, V_i and V_o respectively. One of the meniscus between air and oil, originally flat, becomes unstable when the cylinders rotate faster than a critical value. The complete stability diagram was presented in figure 1 of ref. [3]: the present article being only dedicated to the STI regime (where the cylinders are corotating) and to the very first events where contamination

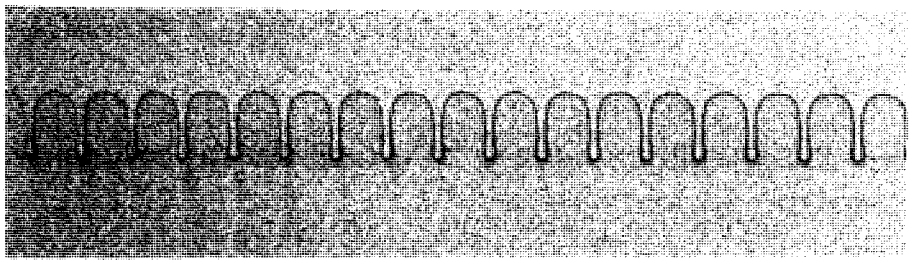

Fig. 1. Photograph of the meniscus, above the instability threshold. Here the inner cylinder is rotating alone and the pattern is stationary.

processes are clearly visible (i.e. one of the two cylinders rotates very slowly). We must first summarize the essential features of the basic steady state which are described elsewhere [3–5].

When only one cylinder is rotating (e.g. $V_o = 0$) and for steady conditions above threshold, the interface is static and periodic in space. The pattern is formed of identical cells in which air penetrates the oil. This cells are sinusoidal near the bifurcation threshold, deep and similar to Saffman–Taylor fingers far from it [8]. These cells are then separated from each other by an oil wall (fig. 1). Their shape can be characterized by Γ, the ratio of the length of the oil wall to the wavelength. In the present geometry, Γ can vary from 0 to 6 depending on the rotation rate. In contrast with related experiments of directional solidification [9–11], the wavelength dispersion at a given velocity is here very small [4] and the phase pinning of the structure on the boundaries is soft. The selected wavelength λ is a unique and decreasing function of the rotation rate of the cylinder. We will call this cellular pattern the ordered state.

3. The regime of spatio-temporal intermittency

If now the other cylinder is set into rotation ($V_o > 0$ and $V_o \ll V_i$), the cellular pattern looses its coherence in space and in time. A spatio-temporal representation of this new regime is obtained by observing the time evolution of one video line parallel to the interface which intersects the cells. Dark lines represent the position of the oil walls and time increases from top to bottom. This representation (fig. 2) shows, in a steady regime, the coexistence of two states: an ordered one (vertical lines) and a chaotic one. This chaos is characterized by tilted lines, oscillations, appearance of new lines (i.e. the birth of a cell) and coalescence of two neighbouring lines (ie. the death of a cell). It is worth noting that this coexistence is a general feature and that chaotic domains never appear spontaneously from ordered ones, an essential characteristics of the STI. Because the local processes at work are different, we will describe successively the STI obtained for small and large values of the cell shape parameter Γ.

3.1. Shallow cells behavior

Fig. 2 shows a spatio-temporal evolution of the front for small Γ. The ordered domains are crossed by localized waves traveling at a constant velocity. These waves appear on this picture as strips of tilted lines. These waves correspond for the interface to the fact that a few cells dilate, shift laterally, then shrink and stop. The motion of the cells and that of the wavepacket occurs in opposite directions. Except the fact that here the wavepackets are constant width, they are similar to those observed during transients after a velocity jump in the ordered state ($V_o = 0$) [4]. These waves have also been observed in other 1D experiments such as directional phase transitions at small Γ [9–11] and thermal convection

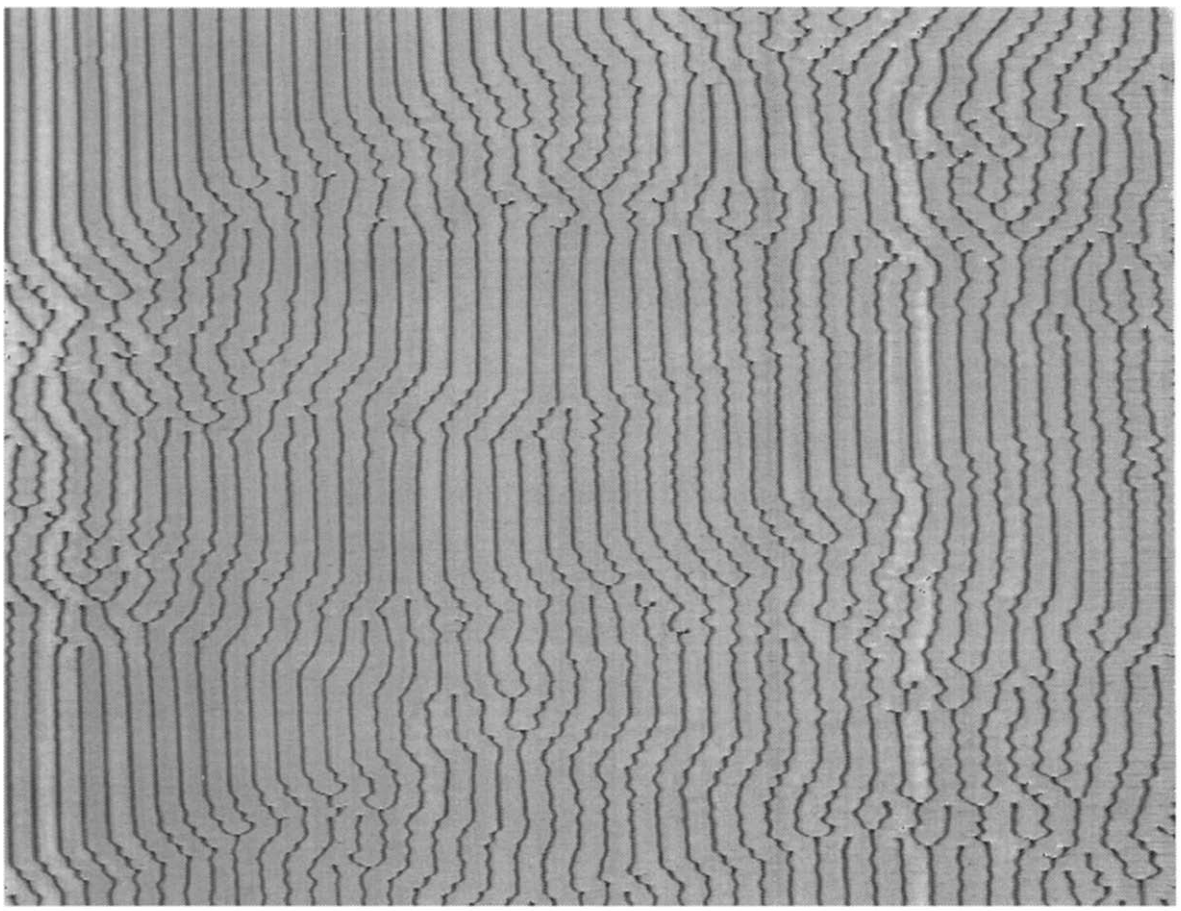

Fig. 2. Space–time picture of the spatio-temporal intermittency regime for a small value of the cell depth ($\Gamma \approx 2.8$). Time elapses from top to bottom in 60 s, $V_i = 260$ mm/s, $V_o = 5.7$ mm/s, and the gap between cylinders $b_o = 0.55 \pm 0.02$ mm.

[2b] (where they have been called solitary modes, tilt waves or parity breaking waves). These waves appear as a result of the spontaneous breaking of the parity of the pattern. A theory presented by Coullet et al. [12] explain them in terms of a bifurcation to an asymmetrical state.

In the present STI regime, the observed waves are always generated by a local and sudden straining of the pattern, and they propagate this localized dilatation. We will therefore call them dilatation waves. These waves can be characterized by the phase slip they impose to the interface (e.g. the phase slip is of the order of 2π in fig. 3). This quantity is not constrained to be quantified but the value π or 2π are frequently observed[#1]. Another important property of such dilatation waves is that, after they passed, the cells retain an out of phase damped oscillation (fig. 3) which can evolve into an optical mode of angular frequency ω. We measure the drift velocity V_d of the dilatation wave along the pattern as well as the optical mode angular frequency ω, for different velocities of the cylinders. Fig. 4a shows, for different V_i, that V_d increases linearly

[#1]This results simply from the creation mechanisms of these waves. The sucking up of a cell at the boundaries creates one wave (with a 2π phase slip); the death of a cell by shrinking off in the middle of the pattern triggers two waves traveling in opposite directions (with a π phase slip).

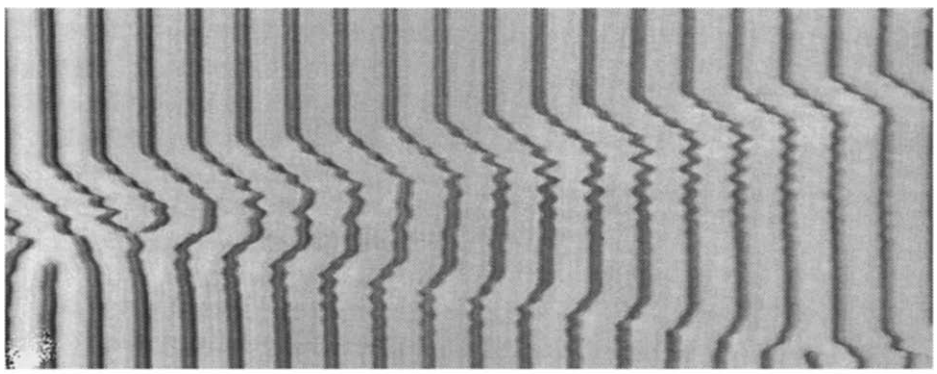

Fig. 3. Spatio-temporal image of a dilatation wave. The wave generates oscillations of the oil walls that are damped in about five oscillations. Time elapses from top to bottom in 20 s, $V_i = 760$ mm/s, $V_o = 2.5$ mm/s, $b_o = 1.10$ mm.

with V_o, the control parameter of the STI transition. Fig. 4b shows the evolution of this drift velocity V_d versus the angular frequency of the optical mode ω. It shows that the dimensionless parameter $V_d/\lambda\omega = 0.4 \pm 0.04$ is constant in all the STI regime.

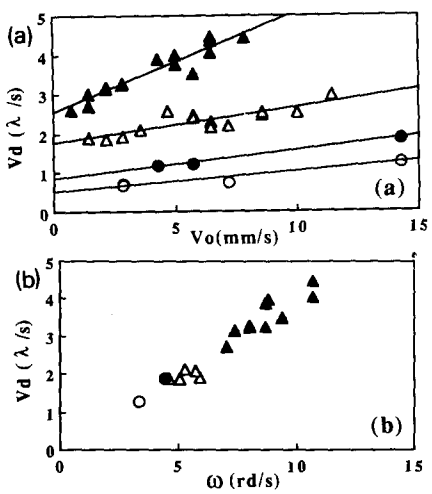

Fig. 4. (a) Evolution of the drift velocity V_d (in wavelength per second) versus velocity of the outer cylinder, V_o, for different velocities of the inner cylinder V_i. (○) $V_i = 100$ mm/s with best fit $V_d(\lambda/s) = 0.51 + 0.05V_o$ (mm/s), (●) $V_i = 120$ mm/s with best fit $V_d(\lambda/s) = 0.85 + 0.07V_o$ (mm/s), (△) $V_i = 200$ mm/s with best fit $V_d(\lambda/s) = 1.8 + 0.08V_o$ (mm/s), (▲) $V_i = 400$ mm/s with best fit $V_d(\lambda/s) = 2.53 + 0.26V_o$ (mm/s).

(b) Evolution of the drift velocity versus ω (angular frequency of the optical mode) for $b_o = 0.55$ mm and for different velocities of the two cylinders.

Let us now describe how these traveling waves propagate disorder. At the beginning of the STI transition, the nucleation of a dilatation wave is a rare event occurring generally at the extremities of the front (when a cell vanishes) and the waves are damped in few wavelengths. For a slightly larger value of the control parameter, the attenuation length becomes large and the waves cross the whole pattern almost unchanged (eventually a wave bounces at the extremity and crosses again the pattern in the other direction as was also observed in ref. [2b]). There are now more left and right traveling waves which collide, and in the same time, the chaotic state seems to sustain itself longer. The dilatation waves leaves behind oscillations which perturb the ordered state and can revive the chaotic one (fig. 2). The initial contamination of the interface thus comes from the boundaries by these dilatation waves. Once chaotic domains exist, as they contain frequent sudden and localized staining of the pattern (e.g. by a cell death), they in turn create outgoing dilatation waves that propagate disorder far away (fig. 3). The limiting factor to the number of traveling waves is that they disappear by collisions or by nucleation of a new cell (e.g. center of fig. 2). Fig. 2 corresponds to such a regime where many waves exist but with still a low proportion of chaos. A further increase in the outer cylinder velocity increases the propor-

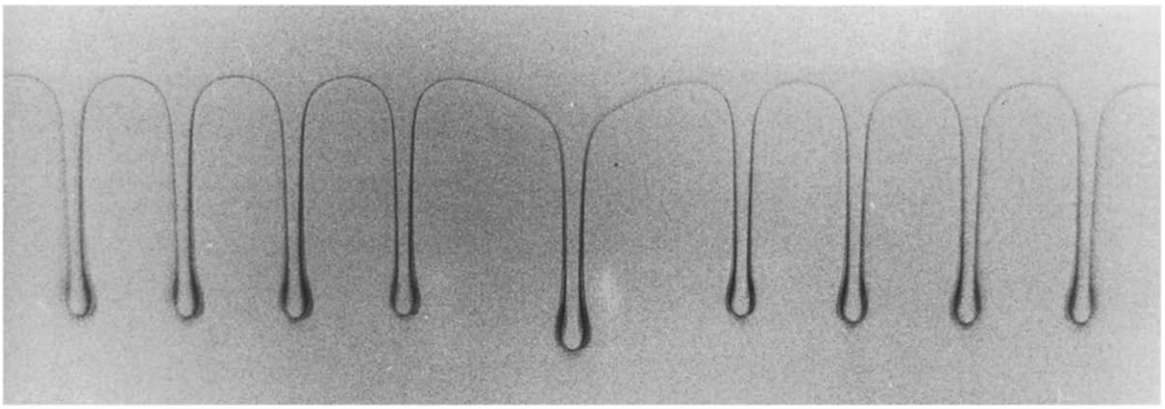

Fig. 5. Picture of an interface showing a pair of asymmetrical cells.

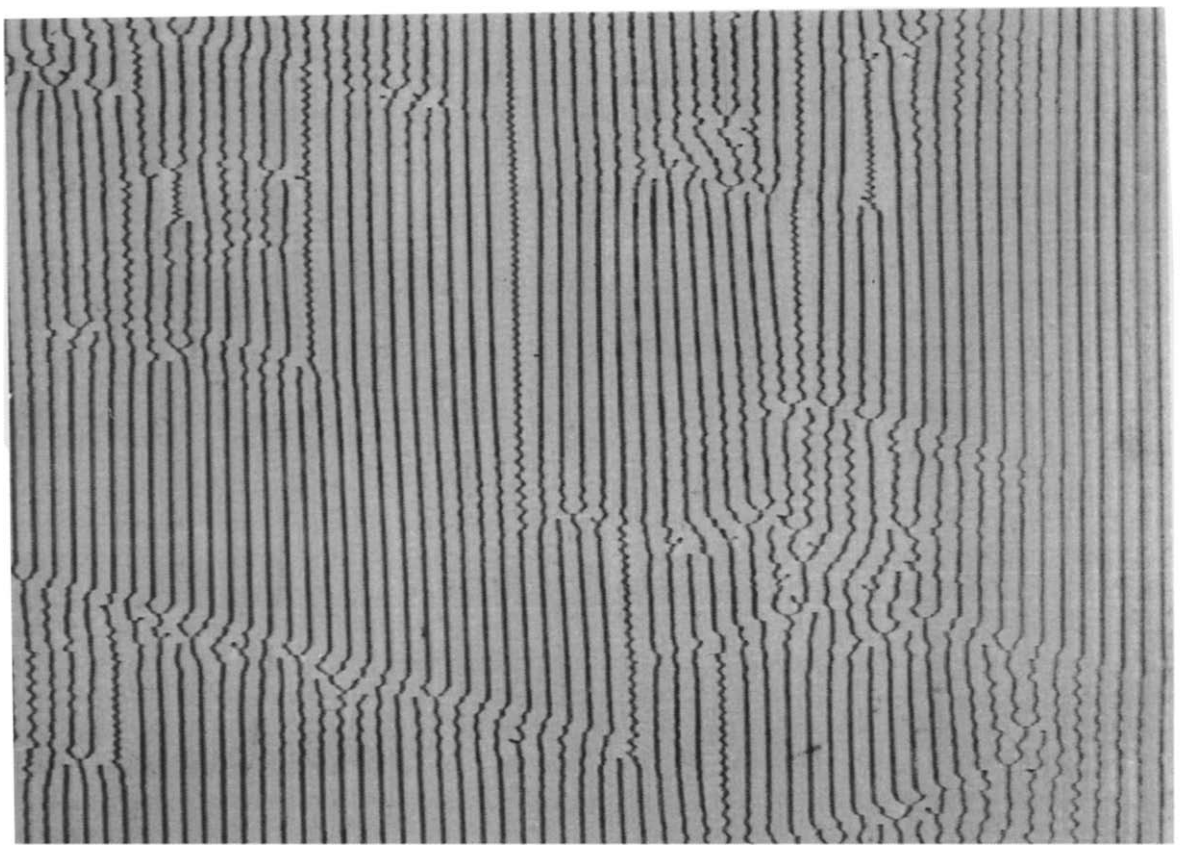

Fig. 6. Spatio-temporal image of the intermittency regime for large cell depth ($\Gamma \approx 3.5$). Anomalous pairs appear as sinuous vertical lines. Their death is clearly visible. Time elapses from top to bottom in 30 s, $V_i = 530$ mm/s, $V_o = 3.1$ mm/s, $b_o = 0.40$ mm.

tion of the chaotic state, and the traveling waves can now only be identified as the incoming front of the chaotic state in the last ordered islands. After this the front becomes fully disordered. Therefore, during the whole STI transition at small cell depth Γ, dilatation waves appear as the basic elementary process of the invasion.

3.2. *Deep cells behavior*

For large depth Γ of the cells, the dilatation waves are damped and a new structure becomes important in the contamination process by the chaotic phase. These defects are pairs of asymmetrical large cells. On the interface they appear as couples of wide asymmetric cells (fig. 5). These defects are motionless, metastable and are usually three basic wavelengths wide. They can be created by symmetrical straining of an oil wall (e.g. by collision of two opposite dilatation waves). Similar objects were observed in other 1D instabilities [2b,10] and in the simulation of the Kolmogorov–Spiegel–Sivashinsky equation [13]. As shown on fig. 6, these pairs either die by splitting into three cells or by slowly shrinking. A characteristic feature of these pairs is the oscillation of their inner wall due to alternate side-branching instability [4] (the frequency of this oscillation is of the order of 1 Hz so comparable to the capillary frequency associated to the wavelength of the pattern). For large pairs, the oscillation frequency is high and the oscillation does not affect the neighbouring cells. If the pair shrinks (e.g. in the middle right of fig. 6), the frequency decreases and the defect disappears by suddenly exciting optical oscillations in its vicinity. Because the lifetime of the static pairs is longer than the current lifetime of chaotic domains, such pairs can be seen as a localized storage of pattern straining which propagates the chaotic state "through" time.

4. Spring model

The localized waves existing in the STI regime for small aspect ratio of the air fingers, suggest an elastic behaviour of the interface. Indeed similar waves would be observed in a linear array of coupled masses with a link between nearest neighbours by a string of stiffness k:

$$\frac{d^2x_n}{dt^2} = \frac{k}{m}(x_{n+1} + x_{n-1} - 2x_n),$$

where x_n is the abscissa of a point of mass m. In fig. 7 we simulated the time evolution of such system when one extremity is abruptly strained to a new position at $t = 0$ (this displacement is then the initial phase slip of the wave). This

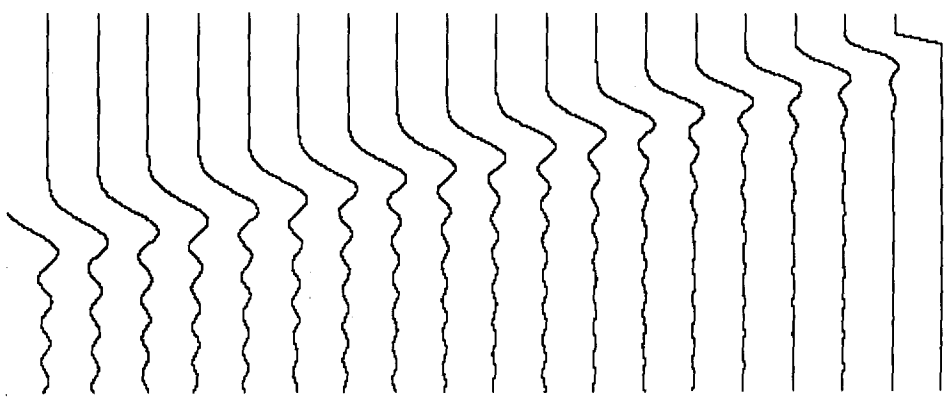

Fig. 7. Numerical simulation of the spatio-temporal evolution of the position of masses linked by springs after an abrupt shift of 1.2 wavelength of the rightmost mass (time elapses from top to bottom).

figure shows that dilatation wave then propagates (at a given group velocity $V_g = a(k/m)^{1/2}$ where a is the initial distance between mass) and that an optical oscillation (of angular frequency $\omega = 2(k/m)^{1/2}$) can be excited. There is strong similarity with fig. 3, even though in this simulation there is a small dispersion of the wave and no dissipation. The characteristic dimensionless parameter is $V_g/a\omega = 0.5$ which is near the experimental value of 0.4 found in all the STI domain. Naturally this linear equation is insufficient to properly describe the effects of this waves (e.g. it cannot describe cells nucleation process and it allows compression waves that are never experimentally observed) but this model shows that there is an elastic constant of the pattern and that is value can be determined by measuring the drift velocities.

For deep cells (large Γ) the dynamics of the death of asymmetrical pair of cells can also be interpreted as an elastic behaviour. In order to excite a collective mode the frequency of the inner wall oscillation must reach the frequency of an optical mode oscillation. This is again similar to the low pass filter behaviour of an array of coupled masses.

So in both cases an elastic behaviour of the pattern exist. It is worth noting that an elastic behaviour was also found by Frisch et al. [14] in the one dimensional equation of Kuramoto–Sivashinsky which is known to present also a regime of spatio-temporal intermittency.

5. Conclusion

In this work, we demonstrate experimentally the existence of two types of localized structures in the transition to chaos of the printer instability. Both kinds of objects, dilatation waves and asymmetrical pairs of cells, are generated by local and sudden straining of the pattern, and appear as the agents of the contamination of the ordered domains by the chaotic ones. Dilatation waves propagate phase defects along the front while asymmetrical cells freeze them for a time before suddenly releasing them.

Because they are seen in various systems (experimental and numeric) the two structures described in this article seem to be robust ingredients for the transition to chaos of one dimensional pattern forming systems. Among the remaining open questions for this class of transitions, we believe the following are important:

– Are these structures the only possible elementary carriers of contamination?

– Does underlying elastic behaviour of the pattern exist for other one dimensional system exhibiting a STI transition to chaos?

Acknowledgements

It is a pleasure to thanks H. Chaté, V. Croquette, H. Cummins, J. Gollub and V. Hakim for useful discussions and Y. Couder and H. Thomé for permanent cooperation.

References

[1] H. Chaté and P. Manneville, Phys. Rev. Lett. 58 (1987) 112.
[2] (a) S. Ciliberto and P. Bigazzi, Phys. Rev. Lett. 60 (1988) 286; (b) F. Daviaud, M. Bonetti and M. Dubois, Phys. Rev. A 42 (1990) 3388.
[3] M. Rabaud, S. Michalland and Y. Couder, Phys. Rev. Lett. 64 (1990) 184.
[4] M. Rabaud, Y. Couder and S. Michalland, Eur. J. Mech. B/Fluids 10 no. 2-Suppl., (1991) 253.
[5] V. Hakim, M. Rabaud, H. Thomé and Y. Couder, in: New tends in Nonlinear Dynamics and Pattern Forming Phenomena: The Geometry of Nonequilibrium, eds. P. Coullet and P. Huerre (Plenum Press, New York, 1990) p. 327.
[6] E. Pitts and G. Greiller, J. Fluid Mech. 11 (1961) 33.
[7] G.I. Taylor, J. Fluid Mech. 16 (1963) 595.
[8] M. Rabaud and V. Hakim, in: Instabilities and Nonequilibrium Structures III, eds. E. Tirapegui and W. Zeller (Kluwer, 1991) p. 217.
[9] J.-M. Flesselles, A.J. Simon and A.J. Libchaber, Adv. Phys. 40 (1991) 1.
[10] S. de Cheveigné and C. Guthmann, J. Phys (Paris) I 2 (1992) 193.

[11] G. Faivre, S. de Cheveigné, C. Guthmann and P. Kurowski, Europhys. Lett. 9 (1989) 779;
J. Bechhoefer, A. Simon, A. Libchaber and P. Oswald, Phys. Rev. A 40 (1989) 2042.
[12] P. Coullet, R.E. Goldstein and G.H. Gunaratne, Phys. Rev. Lett. 63 (1989) 1954.
[13] H. Chaté and B. Nicolaenko, New trends in Nonlinear Dynamics and Pattern Forming Phenomena: The Geometry of Nonequilibrium, eds. P. Coullet and P. Huerre (Plenum Press, New York, 1990) p. 215.
[14] U. Frisch, Z. Su She and O. Thual, J. Fluid Mech. 168 (1986) 221.